NASA-CR-196395

MCAT Institute
Progress Report
94-23

Instabilities Originating from Suction Holes used for Laminar Flow Control (LFC)

Jonathan H. Watmuff

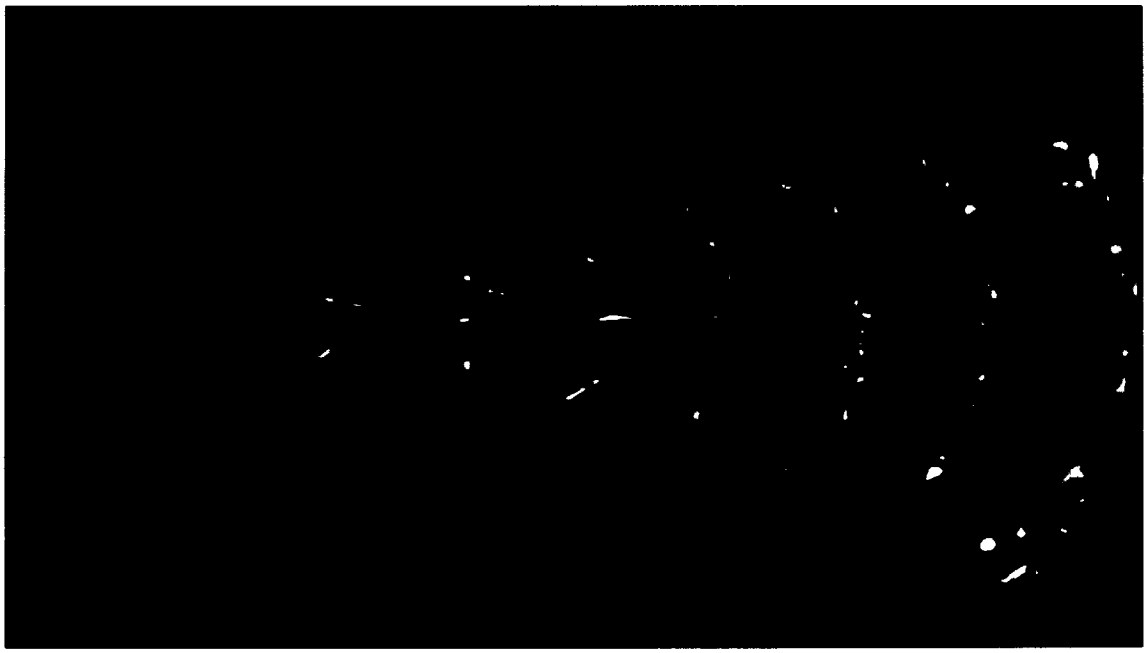

July 1994

NCC2-698

MCAT Institute
3933 Blue Gum Drive
San Jose, CA 95127

Instabilities Originating from Suction Holes used for Laminar Flow Control (LFC)

MCAT Institute
Progress Report 94-23, July 1994

Contract NCC2-698

Jonathan H. Watmuff

SUMMARY

A small-scale wind tunnel previously used for turbulent boundary layer studies has been modified for experiments in Laminar Flow Control. The facility incorporates suction through interchangeable porous test surfaces which are used to stabilize the boundary layer and delay transition to turbulent flow. The thin porous test surfaces are supported by a baffled plenum chamber box which also acts to gather the flow through the surface into tubes which are routed to a high pressure fan. An elliptic leading edge is attached to the assembly to establish a new layer on the test plate. A slot is used to remove the test section flow below the leading edge. The test section was lengthened and fitted with a new ceiling. Substantial modifications were also made to the 3D probe traverse.

The facility is totally automated under computer control and can be run continuously (24 hours/day) for weeks at a time. Data is collected on a point-by-point basis and multiple probes have been implemented to reduce the experimental run-time. The results are examined using the software tools developed for studying the results of numerical simulations on a graphics workstation.

Detailed studies have been made using isolated holes to explore the underlying instability mechanisms. The suction is perturbed harmonically and data are averaged on the basis of the phase of the disturbance. Conditions corresponding to strong suction and without suction have been studied. In both cases, 3D contour surfaces in the vicinity of the hole show highly three-dimensional T-S waves that fan out away from the hole with streamwise distance. With suction, the perturbations on the centerline are much stronger and decay less rapidly, while the far field is similar to the case without suction. Downstream the contour surfaces of the bow-shaped TS waves develop spanwise irregularities which eventually form into clumps. The contours remain smooth when suction is not applied.

Even without suction, the Harmonic Point Source is challenging for CFD e.g. DNS has been used for streamwise growth. With suction, grid resources are consumed by the

hole and this makes DNS even more expensive. Limited DNS results so far indicate that the vortices which emanate from suction holes appear to be stable. The spanwise clumping observed in the experiment is evidence of a secondary instability that could be associated with suction vortices.

A typical porous surface for LFC consists of 0.002" diameter holes with 0.020" grid spacing L, which is too small to resolve disturbances. A 20:1 scale porous test surface has been machined for improved spatial resolution while the L/d is still representative of flight conditions. Designers of porous surfaces use Goldsmith's Criterion to minimize cross-stream interaction. However nothing is known about the streamwise interactions. Results using two holes, aligned but displaced in the streamwise direction, indicate that partial TS wave cancellation is possible, depending on the hole spacing and disturbance frequency. Using DNS for streamwise interaction studies will be prohibitively expensive if linear superposition cannot be used for the multiple holes.

1. INTRODUCTION

The beneficial effects of suction for delaying transition to turbulence have been known for some time but it is only recently that the technology has become available to produce large sheets of perforated material for use in aircraft wings at reasonable cost. Flight tests have been conducted recently using porous surfaces containing around 10^9, 0.002 inch diameter laser drilled holes. The drag reduction obtained by maintaining laminar flow over a substantial portion of the wing surface potentially offers considerable fuel savings. Suction, as a means for Laminar Flow Control is being seriously considered for production aircraft in the near future.

Even the most sophisticated engineering design tools for predicting the transition location assume that the suction is uniform. In some cases there is evidence to suggest that the discrepancy between the predicted and observed transition location may be due to local 3D disturbances that are generated by the discrete holes. It is known that a pair of streamwise vortices are generated by a hole when the suction is strong. Designers of porous surfaces use Goldsmith's Criterion to minimize cross-stream interaction between these vortices. However nothing is known about the streamwise interactions that are likely to be even more important. The objective of this project is to determine the characteristics of disturbances generated by suction holes, and whether they decay or amplify with streamwise distance, and the nature of the interactions between disturbances generated by different holes, which are aligned, but displaced in the streamwise direction.

2. MODIFICATIONS TO THE WIND TUNNEL

An existing small scale facility for studying turbulent boundary layers (see Spalart & Watmuff 1993 and Watmuff 1991a) has been modified using Directors Discretionary Funds to create a laminar boundary layer in a Zero Pressure Gradient (ZPG) as the undisturbed base flow.

2.1 Elliptic Leading Edge and Extension to the Contraction

A 2D elliptic leading edge of 24:1 aspect ratio was built to establish a new laminar boundary layer on the test surface which is located on top of the baffled plenum chamber box described below. The surface of the leading edge has been hard anodized and hand polished. The leading edge is located in the free stream, 0.2m downstream of the contraction exit to avoid adverse pressure gradient effects. It is common practice to mount laminar flow test surfaces on legs within the test section and to adjust the stagnation point using a flap attached at the rear. The depth of the plenum chamber box excluded this type of installation so the following alternative was used. Curved sheet metal is attached to the underneath of the leading edge. The sheet metal acts in conjunction with an extension to the contraction exit to form a curved slot for redirecting the excess test section flow (i.e. below the leading edge) out into the laboratory. The relationship between these components can be seen in figure 1.

The presence of the 3D probe traverse causes the test section pressure upstream of it to be slightly higher than the ambient pressure in the laboratory. The stagnation point is set by adjusting the width of the slot which passively controls the flow rate of excess air. Rms velocity fluctuations (u_{rms}) measured with a hot-wire located within the layer downstream was used as a guide for setting the stagnation point. As expected, high levels of unsteadiness were observed when the stagnation point was located below the leading edge (owing to the separation) while the effects were much less dramatic when it was located above. A plot of u_{rms} versus slot width was used to set the stagnation point. The final slot width was selected to correspond to the u_{rms} minimum assuming that this setting corresponds with stagnation point flow.

2.2 Test Surfaces

Typical porous surfaces for LFC consist of 0.002" diameter holes on a 0.020" square grid. This hole size and spacing is too small to resolve flow disturbances. Consequently, this hole size and grid spacing has been scaled up to provide greater spatial resolution for the hot-wire measurements. The test surface consists of 8466 holes, 0.040" in diameter, spaced on a 0.400" grid, which were individually drilled with precision using an NC machine. This 20:1 scaling provides sufficient spatial resolution to follow the evolution of disturbances downstream of the holes while still maintaining a suction geometry length-scale to boundary thickness ratio that is representative of flight conditions. The porous surface was designed to be as wide as possible to minimize contamination from the boundary layers forming over the solid edges. Another impervious test surface was constructed for establishing the base flow and for isolated hole studies. This test surface is identical in all respects to the porous surface described above (with the exception of the suction holes).

2.3 Baffled Plenum Chamber Box

A baffled plenum chamber box is used to gather the flow through the porous surfaces into tubes which are routed to a high pressure fan which acts as the suction source. A critical design objective was to achieve high uniformity of the suction flow rate. The pressure

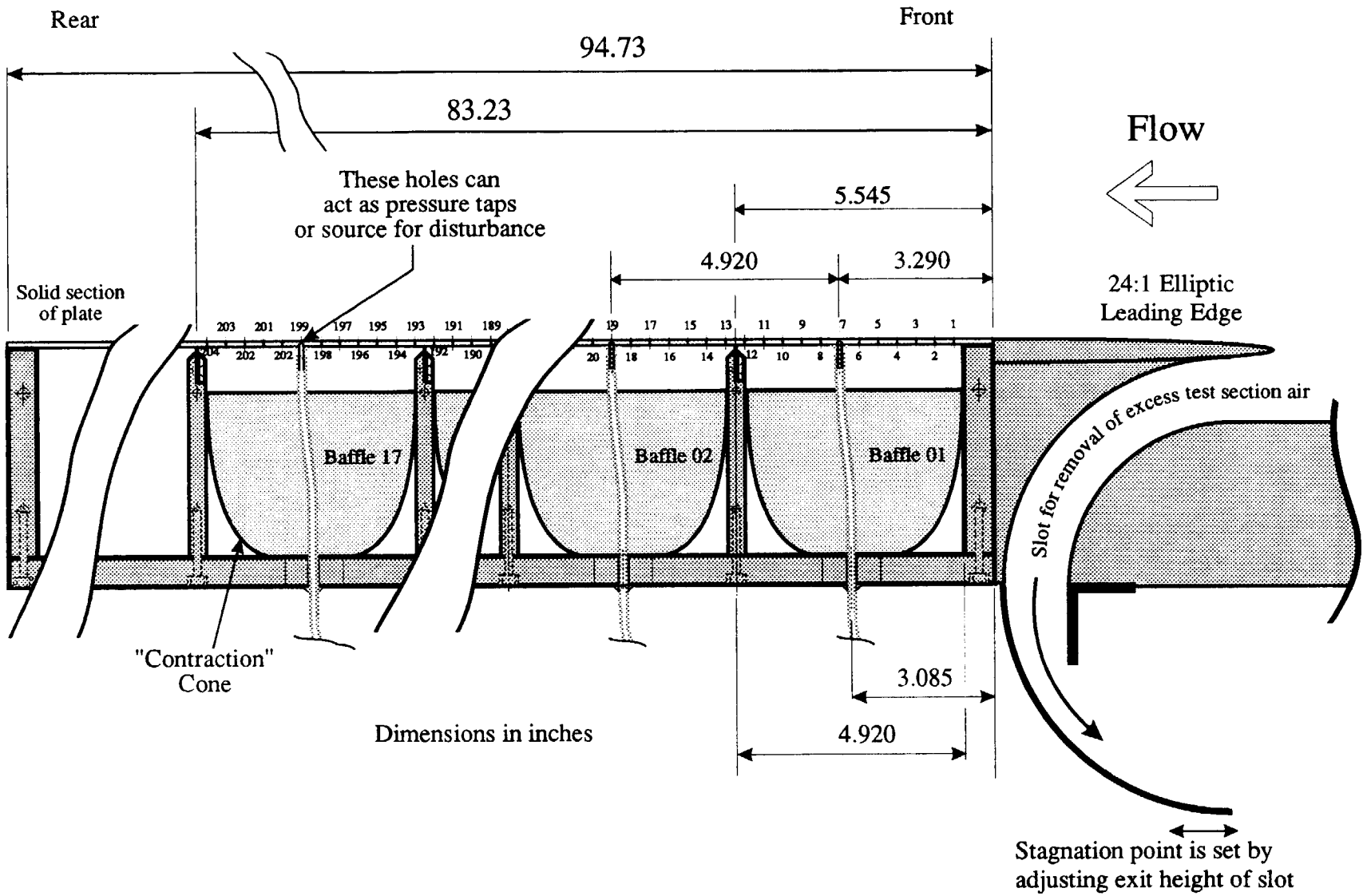

Figure 1. Longitudinal section through test section showing leading edge and baffles for collecting suction flow.

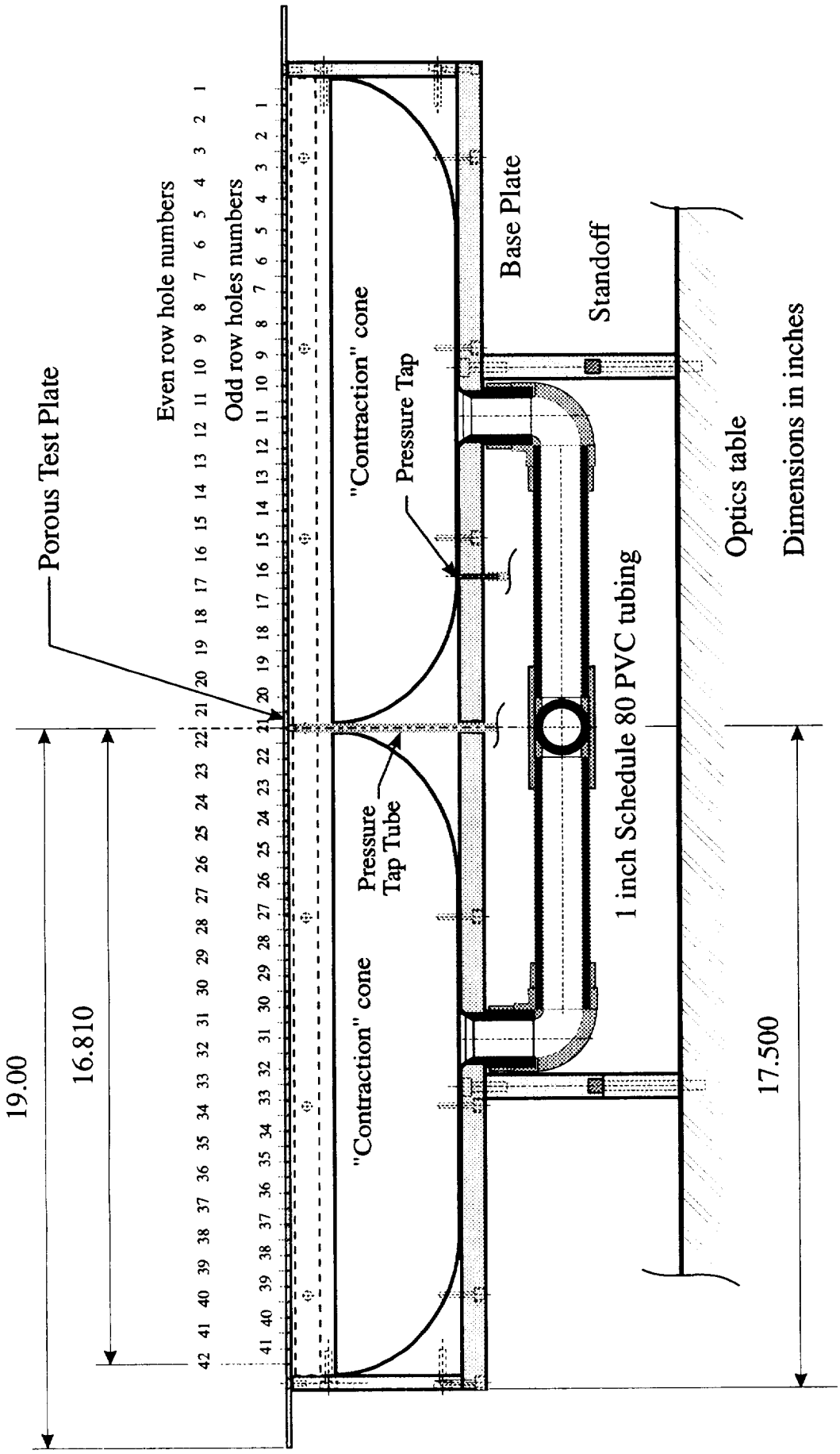

Figure 2. Spanwise cross-section through porous test surface and baffle (view from rear).

differential across the suction surface in the streamwise direction is affected by the pressure drop across the probe traverse. The plenum chamber box is divided into 17 baffles in the streamwise direction to isolate the upstream suction from the presence of the traverse. Another benefit of dividing the box into a number baffles is that the "contraction ratio" is reduced for the flow into the tubes connected to the suction source. As a further means of reducing this contraction ratio, each baffle is subdivided using two inverted bathtub shaped ABS plastic "contraction cones" which were custom built in the Model Shop. The smooth curves of the plastic should also help achieve a steady flow within the baffle.

A longitudinal cross-section through a baffle is shown in figure 1. The internal dividers have 1/16 inch thick stainless steel inserts which provide additional support for the thin porous surfaces. The spacing of the internal dividers is such that none of the 8466 suction holes in the porous test surface is blocked. The flow is gathered from each baffle into two rigid 1" diameter schedule 80 PVC tubes which are joined via a tee below the box. Figure 2 shows a spanwise cross-section through a baffle. The flow from each baffle then continues within a single tube. Routing of these tubes in the confined space beneath the box was performed in situ by softening each tube in turn with a heat gun. Each baffle and the associated tubing system was leak checked prior to installation in the test section. The test surfaces were fixed to the top of the plenum chamber box using "Very High Bond" double-sided tape. This tape is used commercially as an alternative to welding sheet metal and it also ensured leak free joints. Measurements indicated that the deviations of the test surface from a plane were within 0.010".

A Plexiglas model consisting of a single baffle has also been built for checking the spanwise flow uniformity of the suction flow, using water combined with dye flow visualization and hydrogen bubble wires. The model has been used to establish the air flow rate as a function of the pressure differential for a number of porous surfaces. This information was used to select the high pressure fan for suction source.

2.4 New Ceiling, Spacers for Traverse and modifications to Side-Walls

The addition of the leading edge and slot lengthened the test section and a new full length Plexiglas ceiling was manufactured. Turnbuckles are used to adjust the height of the ceiling to set the ZPG. Spacer blocks were used to raise the traverse assembly and the side walls to correctly position them relative to the new height of the test surface above the optics table which forms the base of the test section. Short extensions were made for the sidewalls to complete the test section. The extensions also act as convenient windows providing superior access to the traverse for mounting probes.

2.5 Suction Systems

The 17 tubes routed beneath the plenum chamber box are terminated at a convenient outlet point below the test section. Flexible tubes connect the outlets to 5 micron filters which are located upstream of a bank of flow meters. The filters act as sound and vibration dampers in addition to ensuring that the flow meters are kept clean of contaminants. The flow meters act as convenient visual monitors and are not used for accurate suction flow measurements. Each baffle is fitted with a pressure tap so that the

suction flow rate can be individually calibrated against the pressure differential using the same instrumentation. The internal baffle pressure is used to determine the flow rate under run conditions. Flexible tubes join each flow meter to a common 9" diameter manifold which is connected to a small high pressure blower that acts as the suction source. The flow meters have integral manually adjusted valves which are used to make individual adjustments close to the operating point so that each baffle has the same flow rate . The blower can provide a maximum of 45 inches of water suction pressure which corresponds to individual baffle flow rates of 10 cfm. For a free stream velocity of 20 m/s this corresponds to a $C_q=20 \times 10^{-4}$ which is an order of magnitude greater than typical suction requirements. Therefore flow phenomena generated by over suction can be studied. Because it is a centrifugal fan it does not exhibit undesirable characteristics such as stall or surge at any speed. The fan is driven by a computer controlled dc motor so that the overall suction flow rate can be controlled automatically by simply adjusting the fan speed.

For the isolated suction hole studies the suction source consists of a miniature venturi which is driven by a PID controlled pressure regulator connected to the general purpose compressed air supply of the laboratory. The volume flow rate is calibrated using a high accuracy flow meter while the output of a differential pressure transducer is measured to provide the corresponding set point voltages. During an experimental run various suction flow rates can be applied using the output of a D/A converter of the computer as the PID set point. The suction pressure is then automatically maintained constant by the PID regulator by adjusting the pressure applied to the venturi such that the output of the pressure transducer is equal to the set point.

2.6 Wind Tunnel Fans and Motors

Tests conducted prior to starting the project indicated that a transitional Reynolds number could be achieved using the existing tunnel fan and motor. After completion of the test section modifications it was discovered that the existing 10 HP motor overheated when this flow speed was sustained for long periods. The motor would also be a limiting factor for testing at higher Reynolds numbers required when the porous surface is being used. A new 20 HP d.c. computer controlled motor was procured as a replacement. The original motor now acts as the drive for the high pressure fan which provides the suction.

Power spectral density measurements revealed a spike corresponding to the rotation rate of the fan. This is not too significant since the frequency is well away from the TS wave frequency within the boundary layer. Of more concern was another spectral peak, corresponding to the fan blade passing frequency, which falls within the neutral stability curves for a Blasius layer for a considerable length of the test section. Spectral measurements within the layer also exhibit this peak which appeared to be ultimately responsible for the final transition to turbulence. Unfortunately very little can be done to remove this frequency component from the free stream and the TS wave frequency follows the spectral peak as the fan speed is varied. Further tests revealed that the magnitude of the spectral peaks varied with time in a manner that appeared to be correlated with vibration in the fan. An outside contractor was engaged to balance the fan in situ. This reduced the amplitude of fan vibration and the spectral peaks are subject to much less variation over long periods.

3. EXPERIMENTAL TECHNIQUES

A sophisticated high-speed computer-controlled 3D probe positioning system is integrated into the wind tunnel test section. The traverse is synchronized with a high-speed data acquisition and processing capability and all experimental procedures are totally automated under computer control (Watmuff 1991a). Considerable enhancement of the existing software and hardware were required specifically for this project. Special algorithms were developed to maximize the processing speed (see Watmuff 1994a).

3.1 Modifications to Hot-Wire Probes

The overall size of standard Dantec hot-wire probes was reduced and the prongs were stiffened by bonding a small cross brace with epoxy. The standard 1mm long, 5μm diameter wires were replaced with 0.5mm long 2.5μm diameter wires. The smaller size reduces the disturbance to the flow. Platinum and tungsten are the most commonly used materials for hot-wires. Platinum is resistant to oxidation but its tensile strength is about 1/5 that of tungsten, while tungsten is stronger, but suffers from oxidation at elevated temperatures. Platinum wire is available using the Wollastan process in which a 40μm coating of silver has been deposited on the wire and this helps with probe construction i.e. the raw material is more easily manipulated while soldering onto the prongs. The central region of silver is etched away leaving the sensitive filament. Recently, a platinum coated tungsten wire has become available which combines the best features of each material. A technique was developed for depositing a relatively thick layer of copper to perform the same function as the silver coating with Wollastan wire, so the same manufacturing methods could be used.

3.2 Multiple Probes

Preliminary benchmark tests indicated that the double-buffered data acquisition processing scheme provided a throughput far in excess of the requirements for LFC experiments so tests were conducted using multiple probes. The potential benefit of using multiple probes is that a significant reduction in the total experimental run time can be realized e.g. measurements requiring a 28 day continuous run with a single probe would take only 4 days if 7 probes were used, provided that the processing did not act as a bottleneck. To minimize this problem the high level run-time processing code was "in-lined" by hand. For single probes, an indefinitely sustainable throughput of around 75kHz for a normal wire and 35kHz for a crossed-wire can be obtained for broad band mean velocity and rms fluctuation measurements. The throughputs are reduced to 50kHz and 23kHz respectively when the data is phase-averaged because of the overhead incurred by the sorting. With multiple probes the overall throughput is further reduced because of the extra overhead required for calculation of array indices e.g. the combined rate is 45kHz for multiple normal hot-wire broad band data. This real-time data processing throughput was still considered to be high enough to warrant physical implementation of multiple probes.

A multiple probe holder was constructed in the machine shop for the normal wires and for the crossed-wires. The holders accept standard Dantec probe supports to form a rake of wires with uniform spanwise spacing of 5mm, 10mm or 20mm. Two set screws

are used to make small angular adjustments to the probe support axis. This technique allowed the relative height of each probe to be made collinear within 0.001". Final alignment of the probes with respect to the test surface can then be made by aligning the rake as a whole.

The advantage of using standard Dantec supports is that individual probes can be replaced without having to remove the entire rake from the test section. However, during initial measurements it was discovered that this arrangement created a local adverse pressure gradient which caused separation of the boundary layer. Pressure coefficient measurements were used as a guide for testing mock ups of alternative configurations. The arrangement that produced the least disturbance consisted of thin-walled stainless steel hypodermic tubing projected 6" upstream from the probe holder.

New probes were constructed, in which the only component remaining from the original Dantec system was the small diameter ceramic cylinder used to support the prongs. The replacement probe support consisted of a small tube (with an internal diameter matching the ceramic cylinder) which was "telescoped" inside a larger tube whose external diameter matched the original Dantec probe supports. The tubes were soldered together and a fin was attached for added stiffness. Miniature coaxial cable was soldered directly to the electrical pins of the ceramic cylinder which was bonded inside the probe support and the cable was routed out through the rest of the tubing. No modifications were necessary to the probe holder and the set screws could still be used to adjust the relative height of the sensors, although the method was far more sensitive owing the greater radius arm

The physical layout of the rake of with respect to the traverse restricts the multiple probe measurement grids to being rectangular in the x-z plane. The grid spacing must also be uniform in the spanwise direction but it can be finer than the probe spacing. In this situation the traverse has to perform sequences consisting of a number of small moves equal to the grid spacing, followed by a large move to the position of the first probe at the next grid position. Many other software issues occurred with the implementation of multiple probes but these will not be described here.

3.3 Construction of Constant Temperature Hot-Wire Anemometers

Much effort was spent on the development of new high performance constant temperature hot-wire anemometers for general purpose use in the Fluid Mechanics Laboratory. The design was based on results presented in a series of papers by the author i.e. Watmuff (1987), Watmuff (1988), Watmuff (1989) and Watmuff (1990). Twenty-eight instruments have been delivered, at a cost of around $1K each. The performance is equivalent to commercially available instruments costing $10K each. Nine of these instruments were used in this project. Considerable time was spent this year writing the Contractor Report "A High-Performance Constant-Temperature Hot-Wire Anemometer" which has been submitted for publication (Watmuff 1994b). The analysis and examples of system response have also been accepted for publication, Watmuff (1994c). The design is based on a system theory analysis that can be extended to arbitrary order. A motivating factor was to achieve the highest possible frequency response while ensuring overall system stability. Based on these considerations, the design of the circuit and the

selection of components is discussed in depth. Basic operating instructions are included in an operator's guide. The analysis is used to identify operating modes, observed in all anemometers, that are misleading, in the sense that the operator can be deceived by interpreting an erroneous frequency response. Unlike other anemometers, this instrument provides front panel access to all the circuit parameters which affect system stability and frequency response. Instructions are given on how to identify and avoid these rather subtle and undesirable operating modes by appropriate adjustment of the controls. Details, such as fabrication drawings and a parts list, are provided to enable the instrument to be constructed by others. A number of researchers at Stanford and other outside institutions have already heard of the anemometer and requests for the report have been received even before it is published.

3.4 Phase Pulse and Sine-Wave Generator Circuit

The application of a small sinusoidal sound disturbance through a pressure tapping has been used to generate 3D Tolmien-Schlichtling (TS) waves. A special circuit was built to generate a primary sinusoid in precise synchronization with sampling pulses which are produced at equally spaced phase intervals over the period of the sinusoid. The number of phase intervals can be selected from 16 to 256 in powers of two. As the name suggests, the sampling pulses are used to initiate A/D conversion of hot-wire signals within the boundary layer. The precision offered by the digital circuit removes the phase jitter introduced by instrumentation and allows faster sorting algorithms to be used for data processing. A second sinusoid is generated with a phase-difference that can be set very accurately, either manually or by digital computer. The purpose of the second waveform is to generate another set of TS waves at a hole downstream of the first hole. The interaction between the two sets of TS waves are explored as a function of the phase difference. The amplitude and offset of both sinusoids can be adjusted before the signals are amplified to drive the speakers which produce the disturbances.

3.5 Coprocessor

A perturbation frequency of 145Hz was used for the Harmonic Point Source (HPS) measurements described in section 4.2. The use of 9 probes and 64 phase intervals requires a combined data acquisition processing rate in excess of 80kHz. This processing rate is about 3 times greater than the capabilities of the microVAX 3600 computer. Rather than reduce the number of probes or reduce the phase resolution, a DEC Alpha based coprocessor board was obtained. This unit proved 80 times faster for data processing. However the data must be copied from shared memory to local memory on the coprocessor board to achieve this performance i.e. data flows from the ADC to the microVAX memory at the data acquisition rate and is then copied to the coprocessor. In order for the coprocessor to avoid creating a bottleneck, the combined time for the data transfer to local memory and subsequent processing must not exceed the data acquisition time alone. Even though the Q-bus is considerably slow, by modern standards (i.e. 1.2 Mbyte/s), the increased bus traffic has not proved to be a limitation and the overall data processing rate (including the extra I/O) is in excess of the data acquisition rate.

3.6 Software Enhancements

Experimental run-time code and data-base structures have been written specifically for capturing the evolution of disturbances in 3D space with time. Complex 3D grids containing tens of thousands of data points can be created and experiments performed continuously (24 hours a day) over several weeks without manual supervision. Post-experimental processing schemes are in place for transforming the raw data into the form required to produce animations on an Iris Workstation using the same software tools developed for examining the results of CFD calculations. These tools proved to be indispensable in an investigation by Watmuff (1991b) where a puff was introduced through a hole in the wall to study the evolution of 3D disturbances in a separating laminar boundary layer.

4. RESULTS

4.1 Mean Flow and Broadband Unsteadiness

Transformation of the facility for laminar flow studies has been accomplished with considerable success. The free-stream unsteadiness $u'/U_\infty = 0.08\%$ for a unit Reynolds number $Re_x = 1.25 \times 10^6$ m^{-1} (i.e. a nominal free-stream velocity, $U_\infty = 18.5$ m/s). Intermittent bursting is observed at $x = 1.8$m i.e. $Re_x = 2.25 \times 10^6$, which is very good for an open return wind tunnel. The layer thickness ranges from 2.5mm (0.1 inch) to 4.8mm (0.2 inch) over the measurement range. The mean velocity profiles are shown in figure 3(a) in Blasius coordinates along with the Blasius profile. The conformance with the Blasius profiles is very good and the experimental shape factors for these 16 centerline profiles range from 2.54 to 2.75 compared to the Blasius value of 2.59. The rms velocity profiles are shown in figure 3(b). The peak values vary with $X^{1/2}$ which is an indication of the presence of Klebanoff modes. Very little is known about Klebanoff modes and many workers have spent years trying to rid them from their tunnels. Even after trying obvious techniques, such as cleaning screens, or even buying new ones, these modes often still show up in the boundary layer. Fortunately, they appear to play a passive role because their frequency is so low, but they can also distort the mean flow which could have consequences owing to nonlinear interactions.The skin friction coefficient estimated from the velocity gradient at the wall follows the Blasius C_f vs Re_x distribution within the experimental uncertainty as shown in figure 3(c). The variation the Reynolds number based on displacement thickness with is linear when plotted against $x^{1/2}$, as shown in figure 3(d), along with the Blasius values. No effective origin was used for this plot.

As mentioned in section 2.6, power spectral density measurements within the layer revealed a spike corresponding to the blade passing frequency of the fan. The size of the peak was reduced after the fan was balanced and they are subject to much less variation. By using a slightly lower free stream velocity the measurements near the transition point at revealed that the spectrum is now dominated by naturally occurring TS waves. Tests were also performed in which a small magnitude harmonic disturbance was introduced at a hole in the surface via a speaker to produce a spectral peak of comparable magnitude to the blade passing component. The spectra are essentially identical with and without the disturbance (apart from the spike at the disturbance frequency). These observations

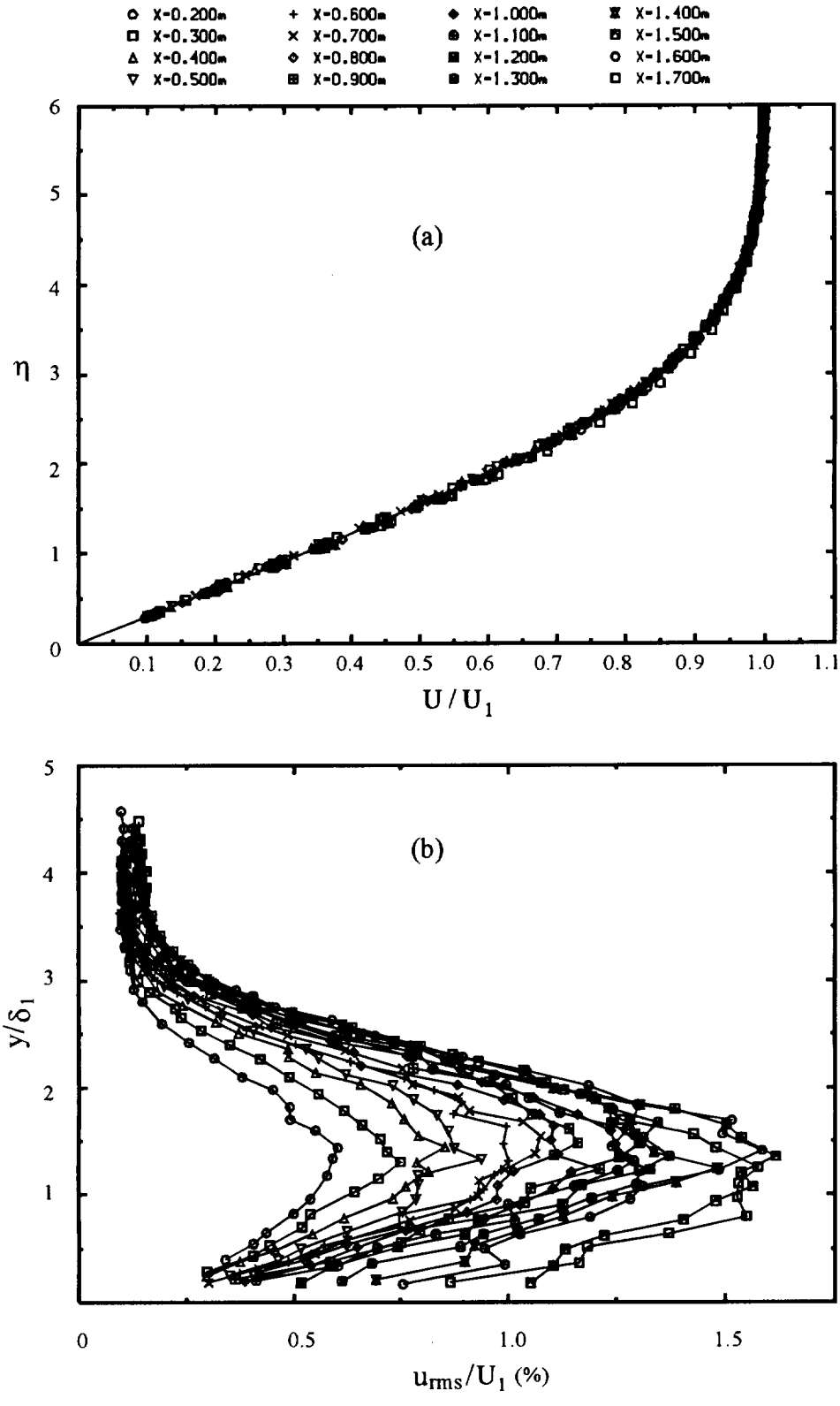

Figure 3. Mean Flow (a) velocity profiles in Blasius coordinates, and (b) rms fluctuation profiles.

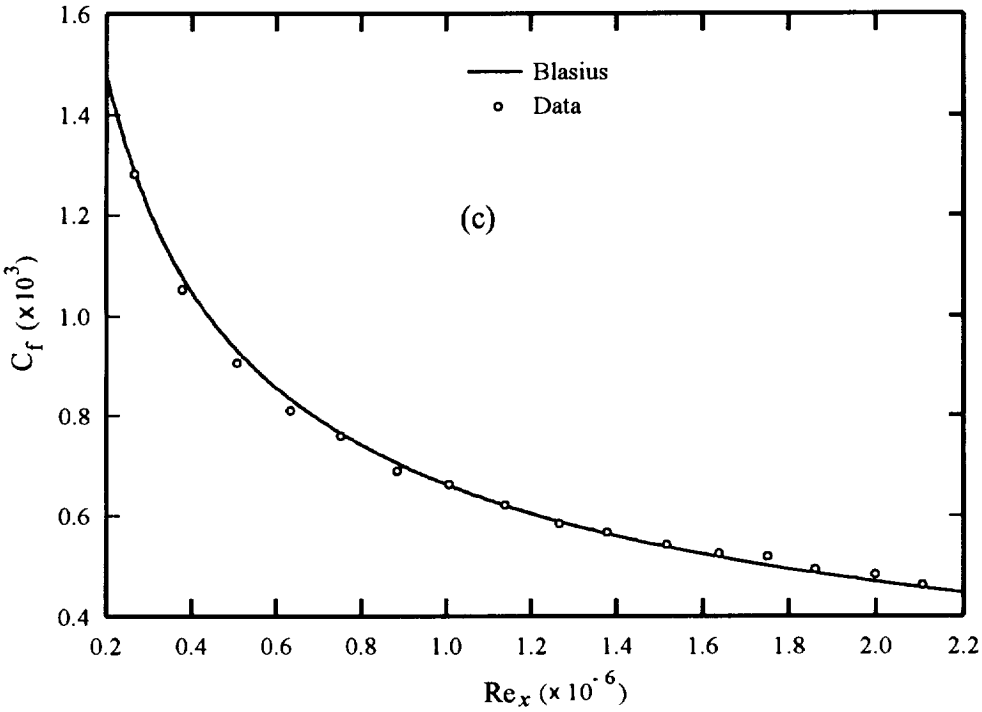

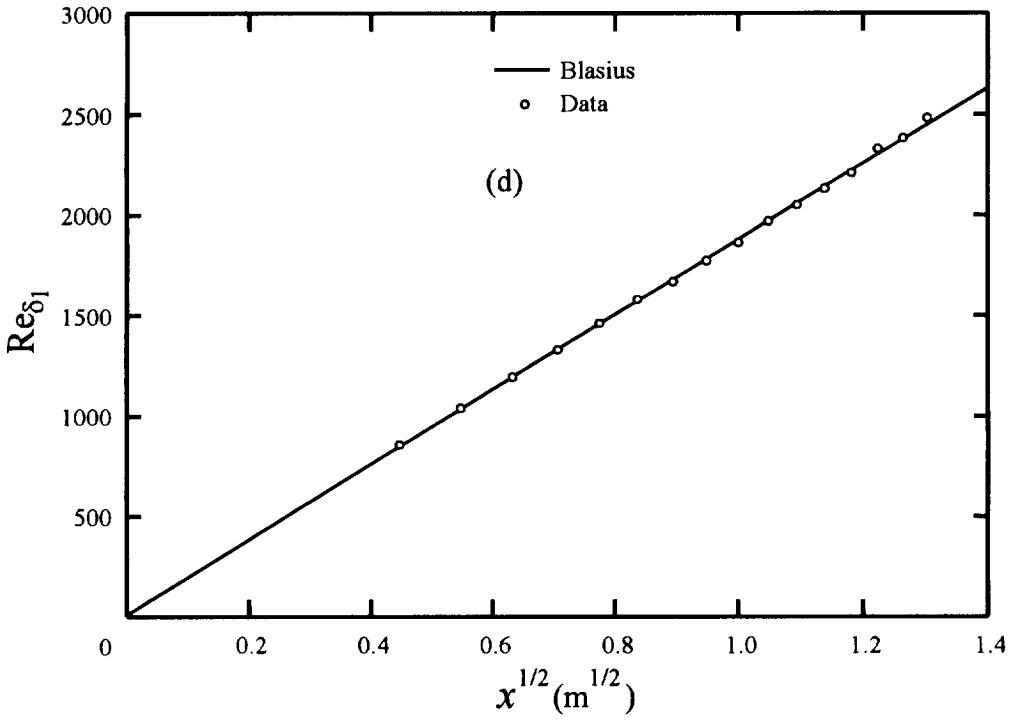

Figure 3 (continued) (c) skin friction from experimental velocity gradient, and (d) variation of displacement thickness

suggest that the disturbance introduced by the passage of the fan blades is linear and of small consequence.

4.2 Single Isolated Hole Studies

These studies are being performed using centerline pressure tap holes in the impervious plate which has been used to verify the acceptability of the base flow. Experiments concerning suction hole disturbances have consisted of the introduction of a harmonic disturbance at an isolated hole via a speaker attached to a pressure tap line as shown in figure 4. The streamwise location of the hole corresponds to $Re_x=1 \times 10^6$, and the nondimensional frequency $F=40 \times 10^{-6}$ corresponds to most amplified mode at this Reynolds number.

Two data sets were obtained on four grids, totaling 79,560 data points each, for the cases without suction and with strong suction ($V/U=0.36$) applied to the hole. Here V is the bulk velocity through the hole and if this hole was embedded in a grid of holes of typical size the suction coefficient would be $C_q \approx 15 \times 10^{-4}$. Multiple probes were used when possible to reduce the experimental run-time. Unfortunately the multiple probes upset the flow and cause local separation of the layer when they are spaced close together. Therefore the use of multiple probes is restricted to measurement grids of large spanwise extent. For example, the first 3D grid, in the vicinity of the hole, contained over 10,000 data points. The small spanwise extent of the grid required the use of a single probe and the measurements took approximately 80 hours of run-time. Further downstream a grid containing around 30,000 data points, required only 24 hours to measure because nine probes could be used.

For both cases (with suction and without suction) the far field evolution of TS waves appear similar, see figure 5. Close to the hole the spanwise propagation of the waves is much smaller than downstream where the spanwise extent appears to grow linearly with streamwise distance being confined to a half-angle of around 12 degrees to the x-axis. The behavior close to the centerline is different in each case. Without suction, the three-dimensionality on the centerline decays with streamwise distance and two-dimensional bow-shaped waves evolve further downstream. When suction is applied to the hole the three-dimensionality is much stronger and does not decay as rapidly. The suction level is sufficiently high for the generation of two streamwise vortices from the hole but the spatial resolution of the probes is insufficient to resolve the details. Further downstream the TS waves develop a "clumpiness" which suggests that the vortices may have become unstable i.e. a secondary instability mechanism is present. A video animation of some of these results was made using NAS facilities with the help of Mrs. V. Hirsch. These results, including the video, were presented at the 46th Annual Meeting of the American Physical Society (Watmuff 1993). The presentation generated considerable interest. Results of DNS calculations for suction holes were also presented by Fasel from the University of Arizona and they clearly showed the breakdown of suction hole vortices.

Two important outside interactions were initiated with computationalists interested in collaboration on aspects of Harmonic Point Source (HPS) disturbances. Professor Thorwald Herbert from Ohio State University is working in conjunction with Dr. Les

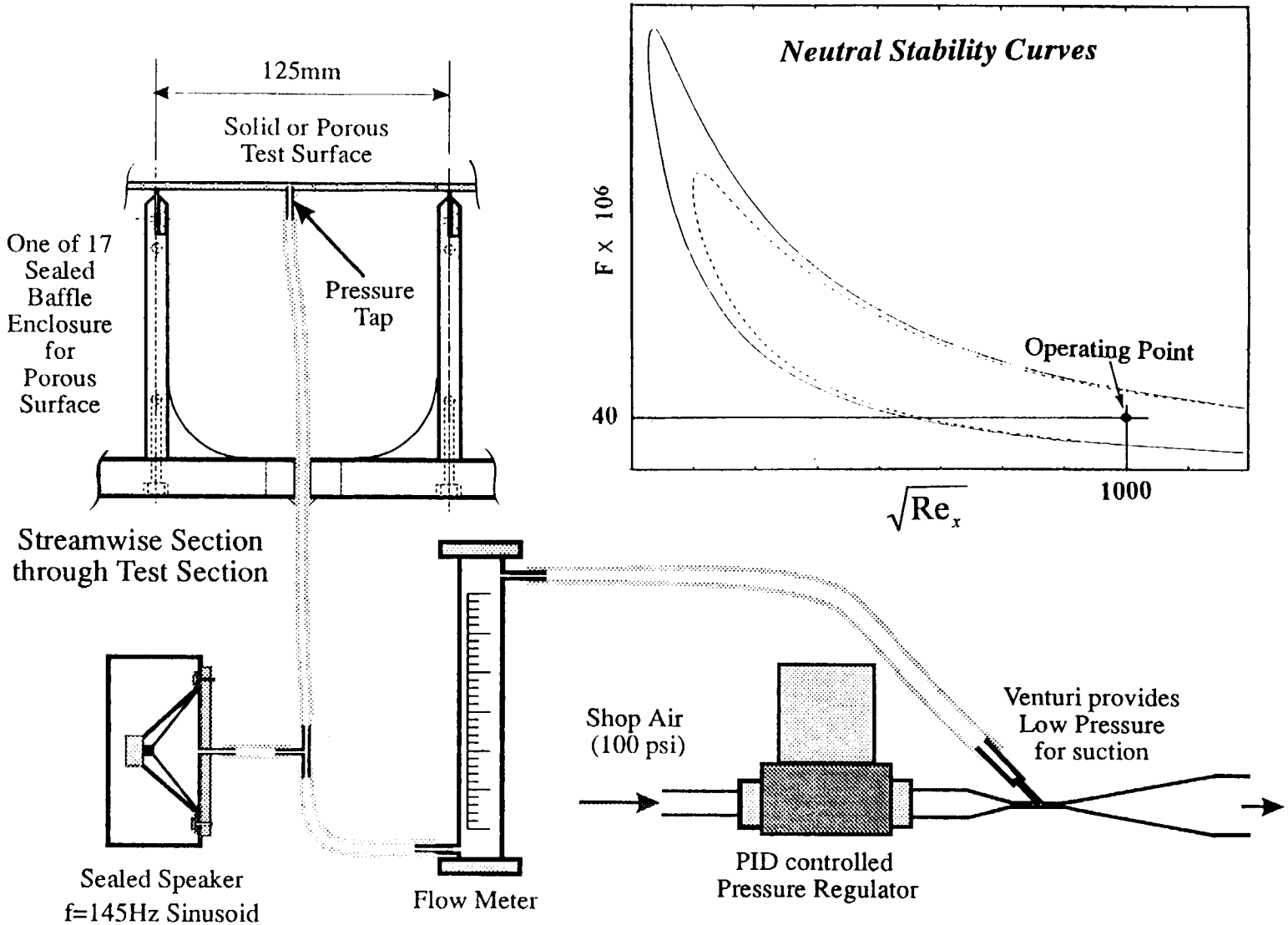

Figure 4.Technique for introduction of perturbation through isolated holes.

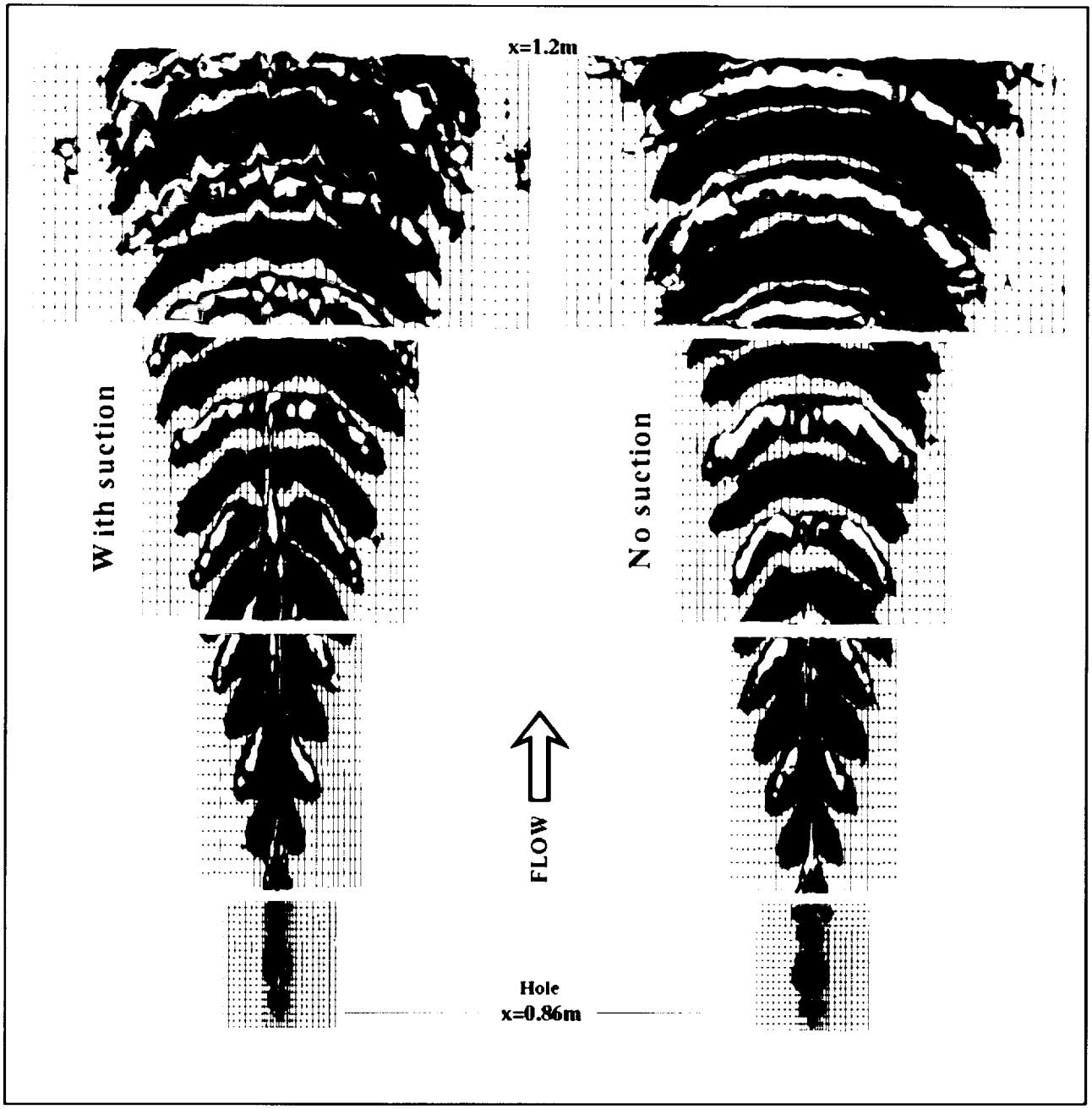

Figure 5. Plan view of 3D contour surfaces of TS waves for cases with and without suction. (Grid for J=1 also shown). Legend: Blue = u / U_1 = - 0.04%, Orange = u / U_1 = + 0.04%. "Clumps" in contours downstream for suction case is evidence of secondary instability that is associated with the suction vortices.

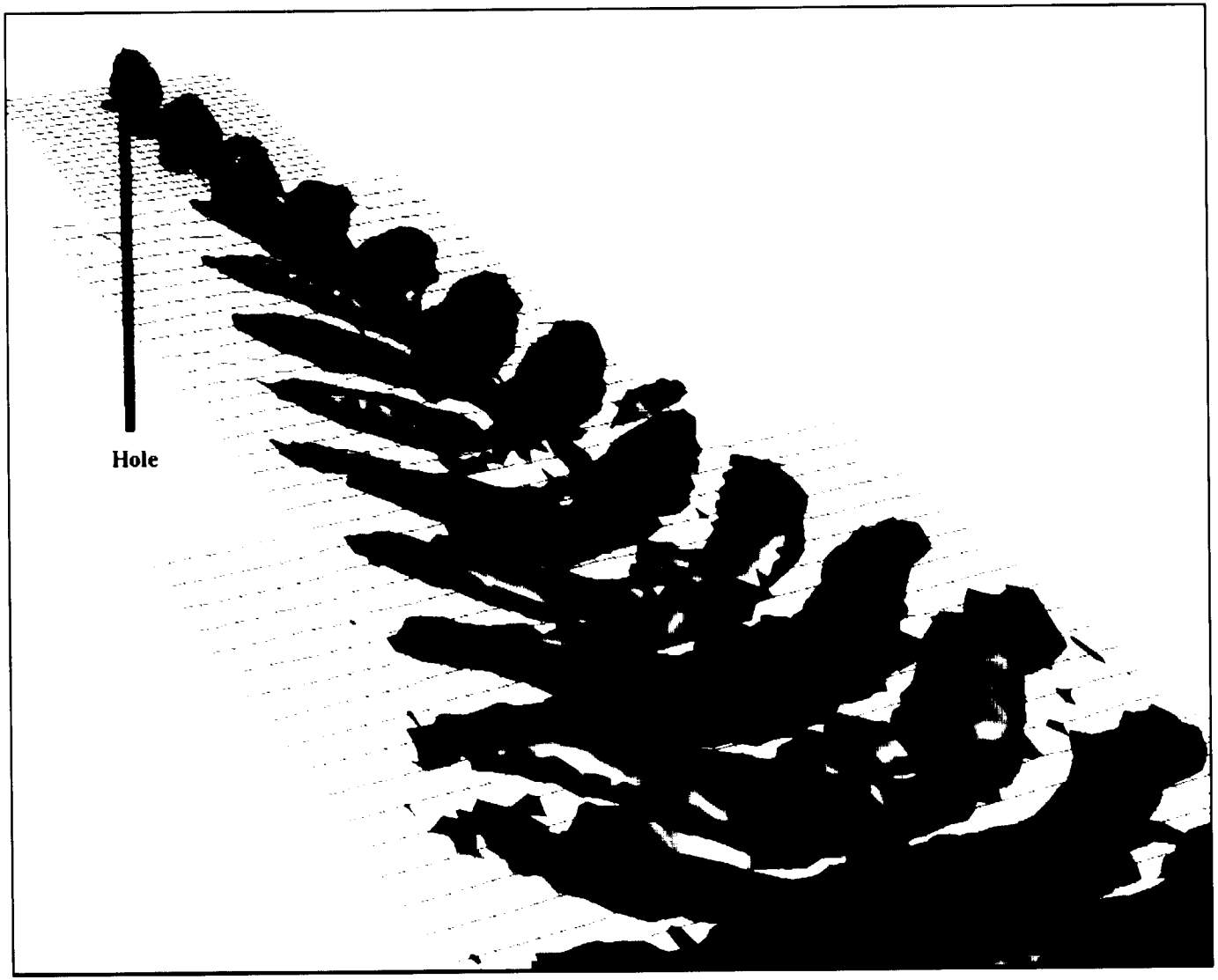

Figure 6. Oblique view of TS waves for case without suction, scaled by factor of 5 in the y-direction normal to surface. (Grid for J = 1 also shown). Legend: Blue (u - U_1) = -0.04%, Orange (u - U_1) = 0.04%.

Mack of JPL on the HPS problem. Dr. Mack is very enthusiastic about the experimental data. He provided references for some earlier quasi-parallel stability calculations he had performed which had been published in an obscure conference proceedings. This work has not been pursued further since that time. The calculations appear to contain many of the detailed features observed in the measurements. Herbert has developed Parabolized Stability Equation (PSE) methods. PSE is more realistic than classical linear stability theory (there is growth in the streamwise direction for example). PSE offers a significant advantage over DNS since only take a few hours on a high performance work station.

Experimental mean flow and perturbation Plot3d files were given to Herbert and Mack and they agreed to a reciprocal exchange of data. Plot3d files were obtained from Thorwald Herbert who is also conducting a DNS investigation of the HPS corresponding to the experimental conditions with no suction. Although these are preliminary calculations, the contour surfaces of u_{rms}/U_∞ have an appearance that is almost identical to the experimental contours, away from the centerline.

However there are major differences on the centerline, especially near the origin of the disturbance. This is not surprising since the HPS was simulated by imposing a time varying velocity component normal to the wall. Currently the simulation is very crude since this boundary condition is imposed at only one grid point. Nonetheless, the implication for DNS is that more sophisticated techniques will be required for modeling the disturbance at, or even within, the hole and potentially this could consume a significant proportion of valuable grid resources.

Dr. L. Mack has provided results from PSE and linear stability calculations corresponding to the case without suction. Again, these results have the same general appearance as the experimental data away from the centerline but contain significant differences in the vicinity of the disturbance.

Dr. L. Mack and Dr. J. Kendall (also of JPL) have suggested that the layer could possess strong Klebanoff modes. Very little is known about Klebanoff modes and many workers have spent years trying to rid them from their tunnels. Even after performing operations, such as cleaning screens, or even buying new ones, these modes often still show up in the boundary layer. Fortunately, they appear to play a passive role because their frequency is so low, but they can also distort the mean flow which could have consequences owing to nonlinear interactions.

4.3 Interactions between disturbances generated at two holes

Interaction between TS waves generated by multiple holes, displaced, but aligned in the streamwise direction is of considerable importance because of the possibility of wave cancellation. Much attention has been given to the *cross-stream* layout of the grid of suction holes (Goldsmith's Correlation) but almost no attention has been paid to the *streamwise* layout of the grids. Initial observations concerning the possibility of wave cancellation were performed using the centerline pressure tap holes of the impervious plate which was used to establish the base flow. Unfortunately the distance between the pressure taps is about three TS wavelengths and the spanwise propagation of the waves

between successive holes is too large to provide a dramatic demonstration of the cancellation. However the tests were successful for demonstrating the linearity of the TS wave interaction which is an underlying requirement for wave cancellation. Three series of tests were performed using two holes. In the first test the harmonic disturbance was applied only to the first hole. In the second test the disturbance was applied only to the second hole and in the third test the same disturbance was applied to both holes. The same spatially dense 3D measurement grid was used in all cases. To demonstrate the linearity the measured perturbations generated by the first hole acting alone were numerically added to the measured perturbations generated by the second hole acting alone. The results constructed from the two sets of independent measurements appeared almost identical to the measurements obtained when the disturbance was applied to both holes simultaneously.

On the basis of these observations, TS wave cancellation was demonstrated using a single set of measurements. Perturbations originating from a second hole located one TS wavelength downstream was simulated by associating the measured perturbations with grid points located downstream. The interaction between disturbances originating from the original hole and the simulated hole was studied by numerically adding the perturbations. The results are shown in figure 6. Wave cancellation in the vicinity of the holes was only minimal owing to the rapid evolution in these regions but further downstream, in the region where the waves become more bow-like, the cancellation of TS waves was extensive. This is an interesting result since it implies that an optimal streamwise hole spacing could exist for cancellation of T-S-wave. The optimum hole spacing would be a function of the flow speed (i.e. TS wavelength).

4.4 Future work - scaled-up fully porous surface.

Typical porous surfaces for LFC consist of 0.002" diameter holes on a 0.020" square grid. This hole size and spacing is too small to resolve the flow disturbances. Consequently, this hole size and grid spacing has been scaled up to provide greater spatial resolution for the hot-wire measurements. A sketch showing the relationship between the holes and a hot-wire probe is shown in figure 6. In follow-on work a 1/8 inch thick stainless steel porous test surface will replace the impervious flat plate. The test surface consists of 8466 holes, 0.041" in diameter, with spaced on a 0.580" square grid which were drilled with precision using an NC machine. The grid was aligned diagonally with respect to the streamwise direction to maximize streamwise distance between the holes. This 20:1 scaling will provide sufficient spatial resolution to follow the evolution of disturbances downstream of the holes while still maintaining a surface length-scale to boundary thickness ratio that is representative of flight conditions.

One simple but potentially dramatic demonstration of oversuction would be to set up flow without suction such that transition is occurring at some streamwise position. The next step would be to turn on mild suction to demonstrate the removal of the transition. The final step would be to increase the strength of the suction such that the transition reappears.

Mean flow and broadband measurements cannot not provide details of what is happening to the suction vortices. Even with the improved spatial resolution, the vortices

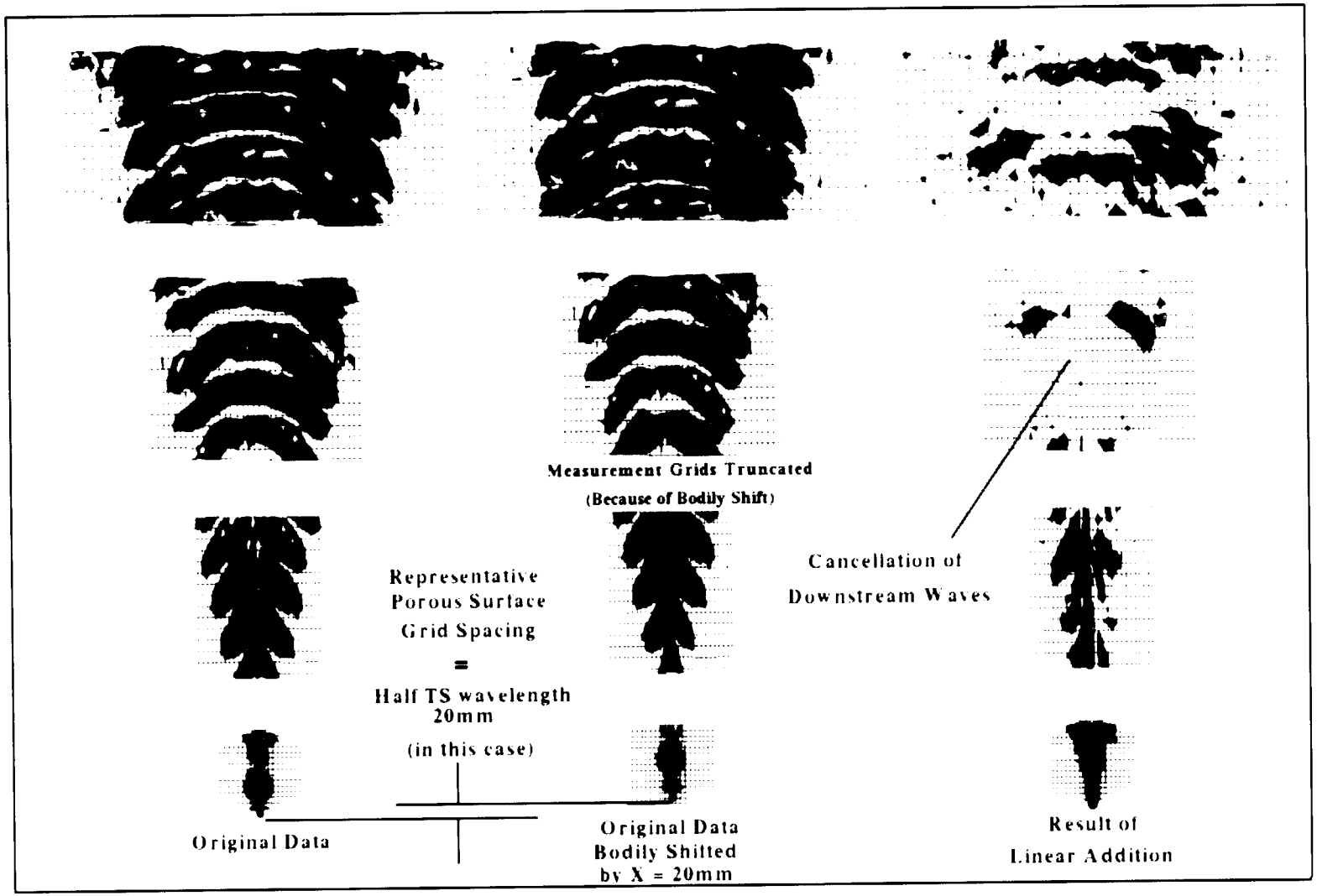

Figure 7. Simulation of cancellation of TS waves using experimental data

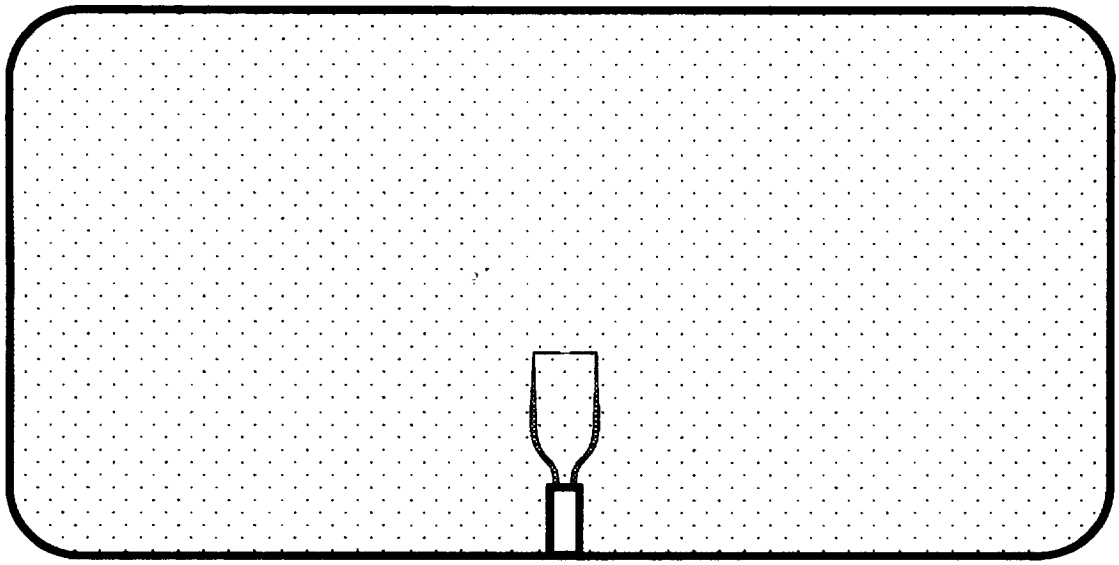

(a)

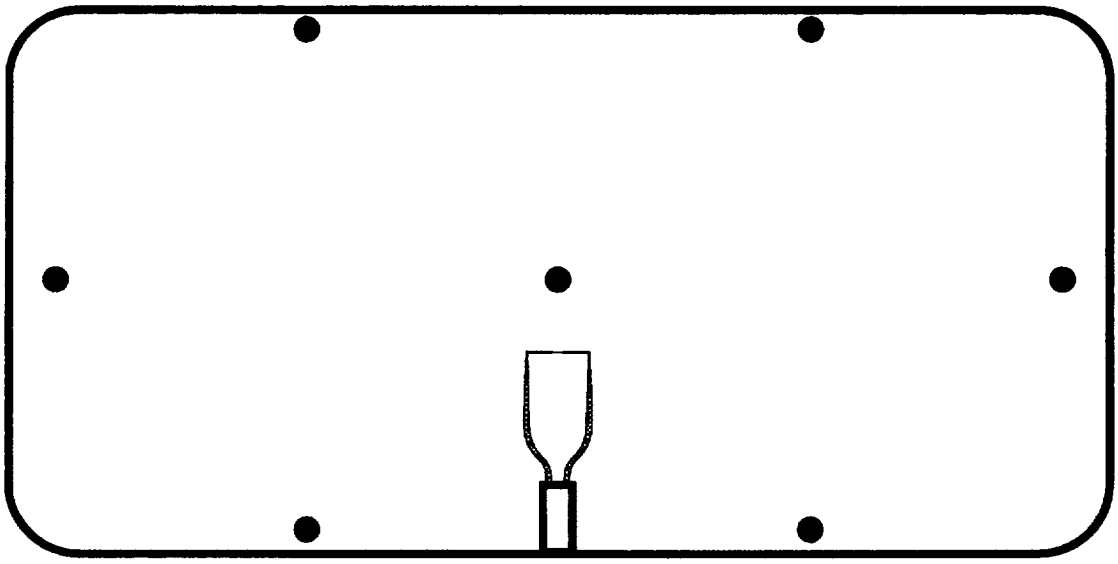

(b)

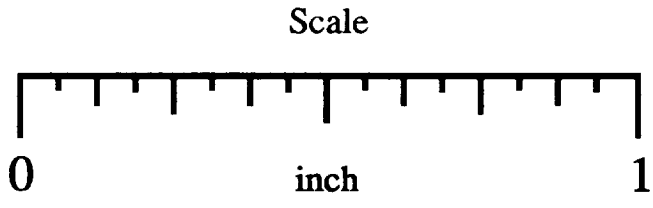

Figure 8. (a) Typical "laser-drilled" porous surface used for flight tests
(b) Typical porous surface scaled up 20:1 for improved spatial resolution with hot-wires

are too small for detailed measurements. However, exciting the vortices by perturbing the suction, as per the isolated hole studies, might reveal some information. While the vortices are too small to see when they are stable, it is anticipated that phenomena, such as secondary instabilities or interactions between the vortices, may be large enough so that details can be extracted using the phase averaging technique.

Some potentially illustrative techniques would include:

(a) Perturbing the suction through a particular hole of the porous surface.

(b) Perturbing the suction through an entire group of holes by using sound in the plenum chamber beneath the surface or a speaker attached to the plumbing system.

(c) Using harmonic perturbations.

(d) Using impulsive perturbations.

REFERENCES

Spalart, P. R. and Watmuff, J. H. (1993) "An Experimental and Numerical Study of a Turbulent Boundary Layer with Pressure Gradients". J. Fluid Mech. Vol 249, pp337-371.

Watmuff, J. H. (1987) "Higher Order Effects in the Frequency Response of the Constant temperature Hot-wire Anemometer". ASME Applied Mechanics, Bioengineering and Fluid Mechanics Conference, Cincinnati, Ohio.

Watmuff, J. H. (1988) "Increasing the Frequency Response of Constant Temperature Hot-wire Anemometer Systems for use in Supersonic Flow". Presented at AIAA 26th Aerospace Sciences meeting, Reno, Nevada.

Watmuff, J. H., (1989) "The effects of Feedback Amplifier Characteristics on Constant Temperature Hot-wire Anemometer Systems". Presented at the tenth Australasian Fluid Mechanics Conference, Melbourne, Australia.

Watmuff, J. H., (1990) "Tuning the Constant-Temperature Hot-Wire Anemometer". Presented at the ASME Symposium on Heuristics of Thermal Anemometry, Ontario, Canada.

Watmuff, J. H. (1991a), "Phase-averaged Measurements of Perturbations Introduced into Boundary Layers". Center for Turbulence Research Annual Research Briefs - Stanford University.

Watmuff, J.H., (1991b) "An Experimental Investigation of Boundary Layer Transition in an Adverse Pressure Gradient", Symposium on Boundary Layer Stability and Transition to Turbulence, First Joint ASME-JSME Fluids Engineering Conference, Portland, Oregon.

Watmuff, J.H., (1993) ``Interaction between instabilities originating from suction holes". Presented at the Forty-sixth Annual Meeting of the American Physical Society, Alburqueque, New Mexico.

Watmuff, J. H. (1994a), "High-speed real-time processing of cross-wire data". Accepted for publication, Exp. Thermal and Fluid Sci. Journal.

Watmuff, J. H. (1994b), "A new high performance constant temperature hot-wire anemometer". NASA Contractor Report (to be published).

Watmuff, J. H. (1994c), "An Investigation of the Constant-Temperature Hot-Wire Anemometer". Paper submitted to Exp. Thermal and Fluid Sci. Journal.